JOURNAL OF THEORETICAL AND APPLIED MECHANICS
42, 4, pp. 719-738, Warsaw 2004

MODELLING OF CREEP-DAMAGE IN THICK PLATE SUBJECTED TO THERMO-MECHANICAL LOADING CYCLES

Artur Ganczarski
Paweł Foryś

Institute of Applied Mechanics, Cracow University of Technology
e-mail: artur@cut1.mech.pk.edu.pl, pforys@cut1.mech.pk.edu.pl

This paper is an extension of the previous authors' papers dealing with the formulation of coupled thermo-creep-damage in 3D rotationally-symmetric structures in the case of combined reverse cyclic mechanical and thermal loads. The thermo-damage coupling is described by the modified Fourier heat flux equation, where the second-rank tensor of thermal conductivity with the damage tensor as an argument is defined. The crack closure/opening effect is incorporated by new effective stress definitions for tension or compression in constitutive equations. It allows for description of incomplete damage deactivation on reverse loading cycles by a new diagonal crack-closure second-rank tensor. Damage evolution is governed by the mixed isotropic/anisotropic Murakami model, modified in order to eliminate non-uniqueness in description of damage growth in the case of rotational symmetry. The creep process coupled with damage is controlled by the Murakami-type equation adapted to reverse cyclic loads. The damage analysis in a 3D plate under thermo-mechanical loadings, which consists in a simultaneous non-homogeneous temperature distribution in the plate over the upper plate originated from the point heat source positioned over the upper plate surface, and the uniform reverse cyclic pressure, is presented as an example.

Key words: thermo-creep-damage coupling, 3D structure, thermo-mechanical loading cycles

List of symbols

$A_1, A_2, n_1, n_2, \overline{\alpha}$	–	constants of Murakami's anisotropic creep law
B, k, l	–	constants of Murakami's anisotropic damage evolution law

B_{ijkl}	–	fourth-rank transformation tensors between eigen and current directions
$\mathbf{D}, \widetilde{\mathbf{D}}$	–	second-rank and fourth-rank damage tensor, respectively
D_{crit}	–	critical damage
E, G, ν	–	Young's and Kirchhoff's moduli, Poisson's ratio
$\mathbf{E}$	–	Hooke's constitutive tensor
h	–	thickness of plate
$\boldsymbol{h}$	–	crack closure second-rank tensor
H	–	Heaviside function
$\mathbf{I}$	–	fourth-rank unit tensor
$\boldsymbol{n}$	–	unit vector normal to wall
$\boldsymbol{n}^{(i)}, \boldsymbol{\nu}^k$	–	unit vector associated with ith or kth principal direction, respectively
p	–	pressure
$\mathbf{P}$	–	fourth-rank projection tensor
$\dot{q}_v$	–	intensity of external heat souce
R	–	radius of plate
t	–	time
t_1	–	cycle length
T, T_{ref}, T_f, T_s	–	temperature, reference temperature, temperature of transition layer and gas temperature of heat source, respectively
$\boldsymbol{u} = [u, w]$	–	vector of displacement in cylindrical coordinates
x	–	distance
$\boldsymbol{x} = [r, z]$	–	vector of cylindrical coordinates
$\mathbf{1}$	–	second-rank unit tensor
α	–	coefficient of thermal expansion
β_0	–	coefficient of free convection
$\boldsymbol{\varepsilon}$	–	strain tensor
λ_0, λ_g	–	coefficient of thermal conductivity, thermal conducticity of gas
$\boldsymbol{\lambda}$	–	second-rank tensor of thermal conductivity
η	–	damage isotropy to anisotropy ratio
$\chi(\boldsymbol{\sigma})$	–	Hayhurst-type isochronous rupture function
$\boldsymbol{\sigma}, \boldsymbol{s}$	–	stress tensor and stress deviator
σ_0, σ_{eq}	–	yield and effective stress
θ	–	temperature change
ζ	–	material parameter of unilateral damage response

and $\widetilde{(\cdot)}$ denotes quantity affected by damage; superscripts e, c, m, th refer to the elastic, creep, mechanical or thermal part of the quantity, respectively; $(\cdot)^*$ – unilateral quantity in which the negative eigenvalues become partly or completely inactive; $(\cdot)^{\pm}$ – positive or negative eigenvalue of the quantity, respectively; $(\cdot)_I$ – Ith eigenvalue of the quantity; $(\cdot)_{eq}$ stand for the effective quantity; $(\cdot)_{\varepsilon,\sigma}$ refer to a quantity whose principal directions coincide with the principal directions of strain or stress, respectively.

1. Introduction

The crucial question arising when a material is subjected to reverse tension-compression cycles is the proper description of a phenomenon of unilateral damage, also called the damage deactivation or the crack closure/opening effect. To this end, the decomposition of stress or strain tensors into positive and negative projections is usually used (cf. Ladeveze and Lemaitre, 1984; Litewka, 1991; Mazars, 1986; Krajcinovic, 1996). In the simplest one-dimensional case, if a loading is reversed from tension to compression, cracks will completely close such that the material behaves as uncracked, or in other words, its initial stiffness is recovered. In a three-dimensional case, modified stress or strain tensors are used based on the concept of the Heaviside functions, where the negative principal components are ruled out

$$\boldsymbol{\varepsilon}_I^* = \langle \boldsymbol{\varepsilon}_I \rangle = H(\boldsymbol{\varepsilon}_I) \qquad \text{or} \qquad \boldsymbol{\sigma}_I^* = \langle \boldsymbol{\sigma}_I \rangle = H(\boldsymbol{\sigma}_I) \quad I = 1,2,3 \tag{1.1}$$

where $\langle a \rangle$ denote McAuley brackets

$$\langle a \rangle = \begin{cases} a & \text{for} \quad a \geqslant 0 \\ 0 & \text{for} \quad a < 0 \end{cases}$$

The above means that the negative principal strain or stress components become completely inactive in the further damage process as long as the loading condition can render them active again (cf. Litewka, 1991). The positive parts of the strain or stress tensors can also be expressed by the use of fourth-order positive projection operators written in terms of the principal directions $\boldsymbol{n}_{\varepsilon}^{(i)}$ or $\boldsymbol{n}_{\sigma}^{(i)}$ (Krajcinovic, 1996; Hansen and Schreyer, 1995) as follows

$$\mathbf{P}_{\varepsilon}^{+} = \sum_{i=1}^{3} \langle \langle \varepsilon^{(i)} \rangle \rangle \boldsymbol{n}_{\varepsilon}^{(i)} \otimes \boldsymbol{n}_{\varepsilon}^{(i)} \otimes \boldsymbol{n}_{\varepsilon}^{(i)} \otimes \boldsymbol{n}_{\varepsilon}^{(i)} \tag{1.2}$$

or

$$\mathbf{P}_{\sigma}^{+} = \sum_{i=1}^{3} \langle\langle \sigma^{(i)} \rangle\rangle \boldsymbol{n}_{\sigma}^{(i)} \otimes \boldsymbol{n}_{\sigma}^{(i)} \otimes \boldsymbol{n}_{\sigma}^{(i)} \otimes \boldsymbol{n}_{\sigma}^{(i)} \tag{1.3}$$

The angular brackets are defined as (Lubarda *et al.*, 1994)

$$\langle\langle a \rangle\rangle = \begin{cases} 1 & \text{for} \quad a \geqslant 0 \\ 0 & \text{for} \quad a < 0 \end{cases} \tag{1.4}$$

whereas $\varepsilon^{(i)}$ and $\sigma^{(i)}$ are principal strain or stress components. Hence

$$\boldsymbol{\varepsilon}^{+} = \mathbf{P}_{\varepsilon}^{+} : \boldsymbol{\varepsilon} \qquad \boldsymbol{\varepsilon}^{-} = \mathbf{P}_{\varepsilon}^{-} : \boldsymbol{\varepsilon} \qquad \mathbf{P}_{\varepsilon}^{-} = \mathbf{I} - \mathbf{P}_{\varepsilon}^{+} \tag{1.5}$$

or

$$\boldsymbol{\sigma}^{+} = \mathbf{P}_{\sigma}^{+} : \boldsymbol{\sigma} \qquad \boldsymbol{\sigma}^{-} = \mathbf{P}_{\sigma}^{-} : \boldsymbol{\sigma} \qquad \mathbf{P}_{\sigma}^{-} = \mathbf{I} - \mathbf{P}_{\sigma}^{+} \tag{1.6}$$

where the corresponding negative or positive eigenvalues of the strain or stress tensors are removed. A more realistic description of the damage deactivation should allow for some influence of the negative principal components of the strain or stress tensors for damage evolution, as observed in brittle materials (cf. Murakami and Kamiya, 1997; Hayakawa and Murakami, 1997). For this purpose, modified strain or stress tensors are defined in principal coordinate systems as follows

$$\boldsymbol{\varepsilon}_{I}^{*} = \langle \boldsymbol{\varepsilon}_{I} \rangle - \zeta \langle -\boldsymbol{\varepsilon}_{I} \rangle = k_{\varepsilon}(\boldsymbol{\varepsilon}_{I}) \boldsymbol{\varepsilon}_{I} \qquad k_{\varepsilon}(\boldsymbol{\varepsilon}_{I}) = H(\boldsymbol{\varepsilon}_{I}) + \zeta H(-\boldsymbol{\varepsilon}_{I}) \tag{1.7}$$

or

$$\boldsymbol{\sigma}_{I}^{*} = \langle \boldsymbol{\sigma}_{I} \rangle - \zeta \langle -\boldsymbol{\sigma}_{I} \rangle = k_{\sigma}(\boldsymbol{\sigma}_{I}) \boldsymbol{\sigma}_{I} \qquad k_{\sigma}(\boldsymbol{\sigma}_{I}) = H(\boldsymbol{\sigma}_{I}) + \zeta H(-\boldsymbol{\sigma}_{I}) \tag{1.8}$$

The additional material parameter ζ in (1.7) and (1.8) describes the unilateral damage response in such a way that for $\zeta = 1$ the unilateral effect is not accounted for, whereas for $\zeta = 0$ the negative principal components do not affect the damage growth. When the general coordinate systems are used, the modified strain or stress tensors are defined in terms of the actual ones by the following mappings

$$\varepsilon_{ij}^{*} = \sum_{i=1}^{3} k(\varepsilon_{I}) n_{iI}^{(\varepsilon)} n_{jI}^{(\varepsilon)} n_{Ik}^{(\varepsilon)} n_{Il}^{(\varepsilon)} \varepsilon_{kl} = B_{ijkl}^{(\varepsilon)} \varepsilon_{kl} \tag{1.9}$$

or

$$\sigma_{ij}^{*} = \sum_{i=1}^{3} k(\sigma_{I}) n_{iI}^{(\sigma)} n_{jI}^{(\sigma)} n_{Ik}^{(\sigma)} n_{Il}^{(\sigma)} \sigma_{kl} = B_{ijkl}^{(\sigma)} \sigma_{kl} \tag{1.10}$$

where the fourth-rank tensors $B^{(\varepsilon)}_{ijkl}$ or $B^{(\sigma)}_{ijkl}$ are built of direction cosines between the principal and current spatial systems (cf. Skrzypek and Kuna-Ciskał, 2003). The above concept is more general than the pure positive and negative projection operators as defined by (1.2) through (1.6). In equations (1.7) and (1.8), the modified strain and stress tensors account for both positive and negative eigenvalues with appropriate weights 1 or ζ. Hence, the equivalent mapping may be furnished by the use of generalized projection operators

$$\mathbf{P}^*_\varepsilon = \mathbf{P}^+_\varepsilon + \zeta_\varepsilon \mathbf{P}^-_\varepsilon \qquad \text{or} \qquad \mathbf{P}^*_\sigma = \mathbf{P}^+_\sigma + \zeta_\sigma \mathbf{P}^-_\sigma \tag{1.11}$$

and

$$\boldsymbol{\varepsilon}^* = \mathbf{P}^*_\varepsilon : \boldsymbol{\varepsilon} \qquad \text{or} \qquad \boldsymbol{\sigma}^* = \mathbf{P}^*_\sigma : \boldsymbol{\sigma} \tag{1.12}$$

In the case when $\zeta_\varepsilon = 1$ or $\zeta_\sigma = 1$, then $\mathbf{P}^*_\varepsilon = \mathbf{I}$ or $\mathbf{P}^*_\sigma = \mathbf{I}$, such that the unique mappings $\boldsymbol{\varepsilon}^* = \boldsymbol{\varepsilon}$ or $\boldsymbol{\sigma}^* = \boldsymbol{\sigma}$ hold. If, on the other hand, $\zeta_\varepsilon = 0$ or $\zeta_\sigma = 0$, then $\mathbf{P}^*_\varepsilon = \mathbf{P}^+_\varepsilon$ or $\mathbf{P}^*_\sigma = \mathbf{P}^+_\sigma$, and $\boldsymbol{\varepsilon}^* = \boldsymbol{\varepsilon}^+$ or $\boldsymbol{\sigma}^* = \boldsymbol{\sigma}^+$ hold.

The limitations of the consistent unilateral damage condition applied to continuum damage theories have been discussed by Chaboche (1992, 1993), Chaboche *et al.* (1995). It was shown that in the existing theories developed by Ramtani (1990), Ju (1989) or Krajcinovic and Fonseka (1981), either non-symmetries of the elastic stiffness or non-realistic discontinuities of the stress-strain response may occur in general multiaxial non-proportional loading conditions. It is easy to show that if the unilateral condition does affect both the diagonal and off-diagonal terms of the stiffness or compliance tensor, a stress discontinuity takes place when one of the principal strains changes the sign and the other remain unchanged (cf. Skrzypek and Kuna-Ciskał, 2003). In the model proposed by Chaboche (1993), only diagonal components corresponding to negative normal strains are replaced by the initial (undamaged) values. The consistent description of the unilateral effect was recently developed by Halm and Dragon (1996, 1998). The authors introduced a new fourth-rank damage parameter $\widetilde{\mathbf{D}}$, built upon the eigenvalues of eigenvectors of $\mathbf{D}$, that controls the crack closure effect with the continuity requirement of the stress-strain response fulfilled

$$\widetilde{\mathbf{D}} = \sum_{k=1}^{3} D_k \boldsymbol{nu}^k \otimes \boldsymbol{nu}^k \otimes \boldsymbol{nu}^k \otimes \boldsymbol{nu}^k \tag{1.13}$$

where the crack-system of the normals $\boldsymbol{nu}^k$ is considered open if the corresponding normal strain is positive (strain-controlled effect).

2. Concept of effective stress accounting for unilateral damage

When the concept of projection operators is applied to constitutive modeling of materials under thermo-creep-damage conditions, the unilateral damage effect may be controlled either by stress or by strain. In what follows, the stress-controlled unilateral damage mechanism is applied.

The distinction between tension and compression in in general 3D case requires the following decomposition of the stress tensor represented by its eigenvalues

$$\boldsymbol{\sigma} = \operatorname{diag}\{\sigma_1, \sigma_2, \sigma_3\} = \boldsymbol{\sigma}^+ + \boldsymbol{\sigma}^- = \langle \boldsymbol{\sigma} \rangle - \langle -\boldsymbol{\sigma} \rangle \tag{2.1}$$

When anisotropic damage is described by the second rank damage tensor represented by its eigenvalues

$$\mathbf{D} = \operatorname{diag}\{D_1, D_2, D_3\} \tag{2.2}$$

and the eigendirections of damage do coincide with the eigendirections of stress, then, in accordance with the concept of the effective stress, the unilateral conditions are written by means of $(\mathbf{1} - \mathbf{D})$ for the positive term and $(\mathbf{1} - \mathbf{D} \cdot \boldsymbol{h})$ for the negative term of (2.1), respectively, then the following modified effective stress for unilateral conditions written in the principal directions (cf. Foryś and Ganczarski, 2002) holds

$$\begin{aligned} \widetilde{\boldsymbol{\sigma}}^* &= \pm\langle \pm\widetilde{\boldsymbol{\sigma}}^{\pm} \rangle \pm \frac{\nu}{1-2\nu}(\operatorname{tr}\langle \pm\widetilde{\boldsymbol{\sigma}}^{\pm} \rangle - \langle \pm \operatorname{tr}\widetilde{\boldsymbol{\sigma}}^{\pm} \rangle)\mathbf{1} \\ \widetilde{\boldsymbol{\sigma}}^+ &= \frac{1}{2}[\boldsymbol{\sigma} \cdot (\mathbf{1} - \mathbf{D})^{-1} + (\mathbf{1} - \mathbf{D})^{-1} \cdot \boldsymbol{\sigma}] \\ \widetilde{\boldsymbol{\sigma}}^- &= \frac{1}{2}[\boldsymbol{\sigma} \cdot (\mathbf{1} - \mathbf{D} \cdot \boldsymbol{h})^{-1} + (\mathbf{1} - \mathbf{D} \cdot \boldsymbol{h})^{-1} \cdot \boldsymbol{\sigma}] \end{aligned} \tag{2.3}$$

in which $\boldsymbol{h}$ stands for the crack closure second-rank tensor represented by its eigenvalues $\boldsymbol{h} = \operatorname{diag}\{h_1, h_2, h_3\}$.

Note, that in the formulation presented above the effect of damage on the Hooke constitutive tensor $\widetilde{\mathbf{E}}(\mathbf{D})$ has been ignored. In the general case, approaching failure $(D_{i_{max}} \leqslant D_{crit})$, this effect may be essential and cannot be neglected. It leads, however, to the necessity of application of damage induced elastic anisotropy, instead of a simplified case of elastic isotropy in the mechanical state equations. The derivatives of the elastic tensor with respect to the space coordinates must be taken into account.

3. Equations of a thick plate subjected to thermo-mechanical loading

In order to apply the above described unilateral damage concept, let us examine the coupled thermo-creep-damage response of a 3D rotationally-symmetric structure subjected to reverse thermo-mechanical loading cycles.

3.1. Assumptions

The displacement and temperature fields fulfil the general rotational symmetry

$$\partial_\varphi \boldsymbol{u} = \boldsymbol{0} \qquad \partial_\varphi T = 0 \tag{3.1}$$

It is postulated that the linearized total strain tensor $\boldsymbol{\varepsilon} = (\nabla \boldsymbol{u} + \boldsymbol{u}\nabla)/2$ may be decomposed into elastic, creep and thermal parts

$$\boldsymbol{\varepsilon} = \boldsymbol{\varepsilon}^e + \boldsymbol{\varepsilon}^c + \boldsymbol{\varepsilon}^{th} \qquad \boldsymbol{\varepsilon}^{th} = \alpha\theta\mathbf{1} \tag{3.2}$$

where $\theta = T - T_{ref}$ and, additionally, the creep part is incompressible

$$\operatorname{tr}\boldsymbol{\varepsilon}^c = 0 \tag{3.3}$$

3.2. Equations of the mechanical state

A coupled thermo-creep-damage formulation is used to describe evolution of a 3D rotationally-symmetric structure subjected to combined thermal and cyclic mechanical loads. The system of mechanical state equations in the displacement formulation is used, where both the creep and temperature terms are included

$$\begin{aligned} &G\nabla^2\boldsymbol{u} + \frac{G}{1-2\nu}\operatorname{grad}(\operatorname{div}\boldsymbol{u}) = \frac{E\alpha}{1-2\nu}\operatorname{grad}\theta + 2G\operatorname{div}\boldsymbol{\varepsilon}^c \\ &\nabla^2 = \operatorname{grad}(\operatorname{div}) - \operatorname{rot}(\operatorname{rot}) \end{aligned} \tag{3.4}$$

where the stress is defined as follows

$$\boldsymbol{\sigma} = 2G\Big[\boldsymbol{\varepsilon} - \boldsymbol{\varepsilon}^c - \alpha\theta\mathbf{1} + \frac{\nu}{1-2\nu}(\operatorname{tr}\boldsymbol{\varepsilon} - 3\alpha\theta)\mathbf{1}\Big] \tag{3.5}$$

It is convenient to decompose the displacement field into purely mechanical and purely thermal parts $\boldsymbol{u} = \boldsymbol{u}^m + \boldsymbol{u}^{th}$. This leads to separation of the

problem described by Eqs (3.4) into two sub-problems in the incremental sense

$$G\nabla^2\boldsymbol{u}^m + \frac{G}{1-2\nu}\,\mathrm{grad}\,(\,\mathrm{div}\,\boldsymbol{u}^{\mathrm{m}}) = 2G\,\mathrm{div}\,\boldsymbol{\varepsilon}^c$$
$$G\nabla^2\boldsymbol{u}^{th} + \frac{G}{1-2\nu}\,\mathrm{grad}\,(\,\mathrm{div}\,\boldsymbol{u}^{th}) = \frac{E\alpha}{1-2\nu}\,\mathrm{grad}\,\theta \tag{3.6}$$

3.3. Modified Fourier equation

The quasi-stationary Fourier equation coupled with damage is applied to describe the damage effect on the heat flux. The effective second-rank tensor of thermal conductivity contains the second-rank damage tensor as an argument

$$\mathrm{div}\,(\widetilde{\boldsymbol{\lambda}}\cdot\,\mathrm{grad}\,T) = 0 \qquad\qquad \widetilde{\boldsymbol{\lambda}} = \lambda_0\,\mathrm{diag}\,\{\mathbf{1}-\mathbf{D}\} \tag{3.7}$$

where λ_0 is the coefficient of thermal conductivity of the initially isotropic material. Only diagonal terms of $\widetilde{\boldsymbol{\lambda}}$ are taken into account (cf. Kaviany, 1995). In this formulation, the effect of unilateral damage is not considered in definitions of the effective tensor of thermal conductivity.

4. Constitutive equations of creep and unilateral damage

A creep process coupled with unilateral damage is controlled by the McVetty-type equation developed by Murakami. It includes the damage effective stress and is extended here to unilateral damage conditions

$$\dot{\boldsymbol{\varepsilon}}^c = \frac{3}{2}[A_1\sigma_{eq}^{n_1-1}\overline{\alpha}\exp(-\overline{\alpha}t)\boldsymbol{s} + A_2\widetilde{\sigma}_{eq}^{n_2-1}\widetilde{\boldsymbol{s}}^*] \tag{4.1}$$

where the modified effective stress deviator

$$\widetilde{\boldsymbol{s}}^* = \widetilde{\boldsymbol{\sigma}}^* - \frac{1}{3}(\,\mathrm{tr}\,\widetilde{\boldsymbol{\sigma}}^*)\mathbf{1} \tag{4.2}$$

includes the crack closure/opening effect Eqs (2.3).

Damage evolution is governed by the anisotropic Murakami model (Murakami *et al.*, 1988), modified by Ganczarski and Skrzypek (2001) in order to eliminate non-uniqueness of the damage growth description in case of rotational symmetry

$$\dot{\mathbf{D}} = B[\chi(\boldsymbol{\sigma})]^k\{\,\mathrm{tr}\,[(\mathbf{1}-\mathbf{D})^{-1}(\boldsymbol{n}^{(1)}\otimes\boldsymbol{n}^{(1)})]\}^l[(1-\eta)\mathbf{1}+\eta\boldsymbol{n}^{(1)}\otimes\boldsymbol{n}^{(1)}]$$
$$\eta = \eta_0\Big[1-\Big(1-\frac{\langle\sigma_3\rangle}{2\langle\sigma_2\rangle}\Big)\frac{\langle\sigma_2\rangle+\langle\sigma_3\rangle}{\langle\sigma_1\rangle}\Big] \tag{4.3}$$

The damage rate is expressed in (4.3) as a linear combination between the isotropic criterion ($\eta = 0$) and the direction determined by the maximum principal stress ($\eta = 1$). In other words, the damage rate is controlled by the reduction of the net area in a plane perpendicular to the direction $\boldsymbol{n}^{(1)}$ of the principal (tensile!) stress σ_1 (exclusively!) combined with the reduction of the isotropic area governed by the Hayhurst-type isochronous rupture function $\chi(\boldsymbol{\sigma}) = a\sigma_1 + b\,\mathrm{tr}\,\boldsymbol{\sigma} + (1-a-b)\sigma_{eq}$. For particular cases $\eta = 0$ and $\eta = 1$, Eqs (4.3) reduces to purely isotropic damage evolution and purely orthotropic microcrack growth in a plane perpendicular to the maximum tensile stress, respectively, whereas for $0 < \eta < 1$ a mixed isotropic/maximum principal stress mechanism of damage growth occurs. Consistently, a simplified representation of the Hayhurst function $\chi(\boldsymbol{\sigma}) = \sigma_1$ is used.

5. Thermo-mechanical boundary problem

5.1. Mechanical boundary problem

A simple support is assumed for the plate under cyclic mechanical load $\pm p$ (Fig. 1). This condition, however, essentially constraints the thermal transverse expansion at the supported edge, so, for the thermal problem, separate boundary conditions are proposed (Fig. 2). Finally, two sets of boundary conditions are used to solve the mechanical problem separately for puerly mechanical and purely thermal loadings (Table 1).

Table 1. Boundary conditions for purely mechanical and purely thermal loads

Boundary	Mechanical load		Thermal load	
top surface	$\sigma_z = \pm p$	$\sigma_{rz} = 0$	$\sigma_z = 0$	$\sigma_{rz} = 0$
bottom surface	$\sigma_z = 0$	$\sigma_{rz} = 0$	$\sigma_z = 0$	$\sigma_{rz} = 0$
symmetry axis	$u_r^m = 0$	$\partial_r u_z^m = 0$	$u_r^{th} = 0$	$\partial_r u_z^{th} = 0$
supported edge	$\sigma_r = 0$	$u_z^m = 0$	$\sigma_r = 0$	$\sigma_{rz} = 0$
lower corner				$u_z^{th} = 0$

5.2. Thermal boundary problem

Assume the point heat source at a distance H above the upper surface. Hence, the temperature distribution of a gas over the upper plate surface is spherically symmetric. Assuming spherical symmetry of the temperature front propagation (Fig. 3a), one may find that the temperature distribution

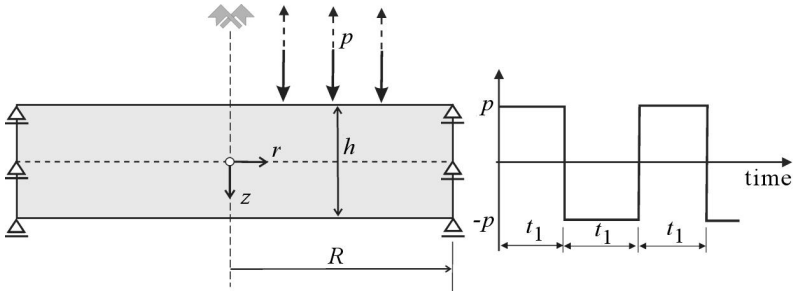

Fig. 1. Boundary conditions for cyclic mechanical $\pm p$ load

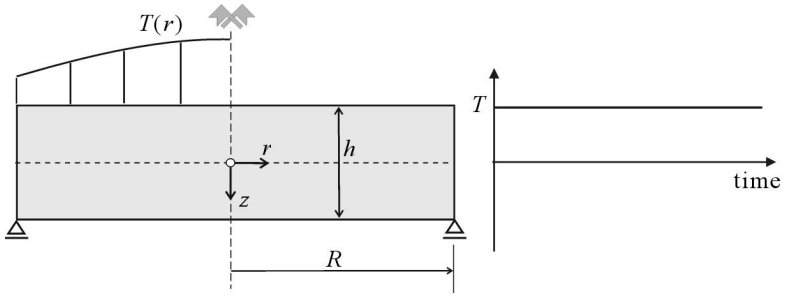

Fig. 2. Boundary conditions for thermal $T(r)$ load

of the gas neighbouring the top surface reveals rotational symmetry and is given by the parabola $T_f(x) = T_s - [\dot{q}_v/(6\lambda_g)]x^2$, where T_s stands for the gas temperature at the heat source, λ_g denotes thermal conductivity of the gas, whereas x is a distance between the heat source and the particle of the gas neighbouring the current point at the top surface.

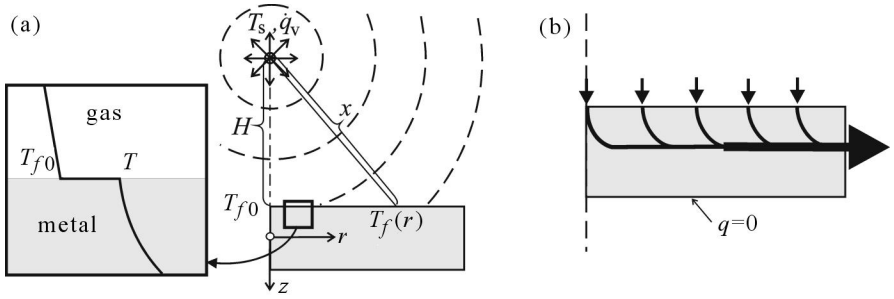

Fig. 3. Temperature front propagation (a) and schematic heat flow through plate (b)

A schematic heat flux through the plate is sketched in Fig. 3b. It is assumed that the whole heat flux, which enters the upper plate surface, goes towards

the supported edge, whereas at the lower surface adiabatic conditions hold. The above assumptions allow one to formulate the mixed and the Neumann integral type boundary conditions for Eqs (3.7) in a following form

$$\begin{aligned}
&\text{upper surface} && \beta_0(1-\mathbf{D}\cdot\boldsymbol{n})(T_f-T) = -\lambda_0(1-\mathbf{D}\cdot\boldsymbol{n})\partial_n T \\
&\text{lower surface} && \partial_n T = 0 \\
&\text{symmetry axis} && \partial_n T = 0 \\
&\text{supported edge} && \int\limits_A [\lambda_0(1-\mathbf{D}\cdot\boldsymbol{n})\partial_n T]\, dA = C
\end{aligned} \tag{5.1}$$

where $\beta_0(1-\mathbf{D}\cdot\boldsymbol{n})$ denotes the damage coupled coefficient of the Newtonian convection between the gas and the upper surface of the plate and $\boldsymbol{n}$ is the unit vector, normal to the wall. The heat flux that enters the top surface of the plate and is sent through the supported edge is kept constant throughout the process ($C = \text{const}$).

6. Numerical algorithm for thermo-creep-damage problem

To solve the initial-boundary problem by FDM, we discretize time by inserting N time intervals Δt_k, where $t_0 = 0$, $\Delta t_k = t_k - t_{k-1}$ and $t_N = t_I$ (macrocrack initiation). Hence, the initial-boundary problems are reduced to a sequence of quasistatic boundary-value problems, the solution to which determines unknown functions at a given time t_k, e.g., $T(\boldsymbol{x}, t_k) = T^k(\boldsymbol{x})$, $\boldsymbol{u}(\boldsymbol{x}, t_k) = \boldsymbol{u}^k(\boldsymbol{x})$ with an appropriate thermo-elastic solution taken as initial conditions. To account for primary and tertiary creep regimes, a dynamically controlled time step Δt_k is required, the length of which is defined by the bounded maximum damage increment

$$\Delta D^{lower} \leqslant \max_{(\boldsymbol{x})}\{\|\dot{\mathbf{D}}^k(\boldsymbol{x}) - \dot{\mathbf{D}}^{k-1}(\boldsymbol{x})\|\Delta t_k\} \leqslant \Delta D^{upper} \tag{6.1}$$

Discretizing also the spatial coordinates $\boldsymbol{x} = [r, z]_{i,j}$, by inserting a mesh $\Delta r = r_I - r_{i-1}$, $\Delta z = z_j - z_{j-1}$, we rewrite equations of heat transfer (3.7) and motion (3.6) for the time step t_k in terms of FDM with respect of r_I and z_j, respectively. Applying a stage algorithm, first for the damage $[\mathbf{D}]_{i,j} \equiv 0$, equation of the thermal problem (3.7) with boundary conditions (5.1) is solved by making use of the procedure `linbcg.for` of Conjugate Gradient Method for sparse system (Press *et al.*, 1993), and the initial "elastic" temperature

$[T^e]_{i,j}$ is found. Then, the system of equations of motion (3.6) with the known temperature field $[T^e]_{i,j}$ as the right hand side and the boundary conditions (cf. Table 1), is numerically solved by the same procedure, and the elastic displacements are determined $[\boldsymbol{u}^e]_{i,j}$ as well. Next, the program enters the creep-damage loop where the damage and strain rates $[\dot{\mathbf{D}}, \dot{\boldsymbol{\varepsilon}}^c]_{i,j}$ are calculated. Repeating again the stage algorithm a solution to discretized thermo-creep-damage problem, rates of temperature $[\dot{T}]_{i,j}$ and displacements $[\dot{\boldsymbol{u}}]_{i,j}$ are computed. In the next time step, the "new" temperature $[T]_{i,j}$ and displacements $[\boldsymbol{u}]_{i,j}$ are found, and the process is continued until the maximum value of damage reaches the critical level $\max[D]_I = D_{crit}$. The failure criterion may be derived from the instability condition of the stress-strain relation $\det(\partial\boldsymbol{\sigma}/\partial\boldsymbol{\varepsilon}) = 0$.

7. Results

7.1. Data

Numerical results presented in this paper deal with plates made of copper of the following thermo-mechanical properties at temperature 523 K (Murakami *et al.*, 1988): $T_{f0} = 300°\mathrm{C}$, $T_{ref} = 0°\mathrm{C}$, $E = 60.24\,\mathrm{GPa}$, $\sigma_0 = 11.0\,\mathrm{MPa}$, $\nu = 0.3$, $B = 4.46 \cdot 10^{-13}\,\mathrm{MPa}^{-k}\mathrm{h}^{-1}$, $l = 5.0$, $k = 5.55$, $\xi = 1.0$, $A_1 = 2.40 \cdot 10^{-17}\mathrm{MPa}^{-n_1}$, $n_1 = 2.60$, $A_2 = 3.00 \cdot 10^{-16}\,\mathrm{MPa}^{-n_2}\mathrm{h}^{-1}$, $n_2 = 7.10$, $\overline{\alpha} = 0.05\,\mathrm{h}^{-1}$, $\alpha = 2.5 \cdot 10^{-5}\,1/\mathrm{K}$, $\lambda_0 = 203\,\mathrm{W/m°C}$, $\beta_0 = 75\,\mathrm{W/m^2°C}$. The loading cycle is defined by the half-amplitude $p = \pm 0.1\sigma_0$ and the cycle length $t_1 = 2000\,\mathrm{h}$. Reverse, Heaviside-type pressure cycles are applied to the structure, whereas temperature of the heat source is kept constant. The characteristic parameter of the plate, i.e. thickness-to-diameter ratio is $h/R = 0.7$. For sake of simplicity, the effect of temperature changes on material constants, and of the damage on elastic moduli are ignored. The parameter which controls the type of damage isotropy-to-anisotropy ratio is $\eta_0 = 0.5$, which means that mixed isotropic/maximum principal stress mechanism of anisotropic damage growth is considered.

7.2. Example

Plate response to mechanical reverse cyclic load $\pm p$

Consider a plate subjected to pure mechanical reverse cyclic load $p = \pm 0.1\sigma_0$. A constant, temperature field $T = 250°\mathrm{C}$ is uniformly applied

to the structure volume, such that the homogeneous thermal strain field does not affect the stress field. The plate is subjected to symmetric, reverse uniform pressure loading cycles applied to the top surface of the plate (Fig. 1). The external heat source is not active in this case.

Following the symmetric loading cycles, the most damaged zones develop at the top and bottom plate surfaces around the symmetry axis. The final distribution of the dominant hoop damage component D_φ at failure is presented in Fig. 4.

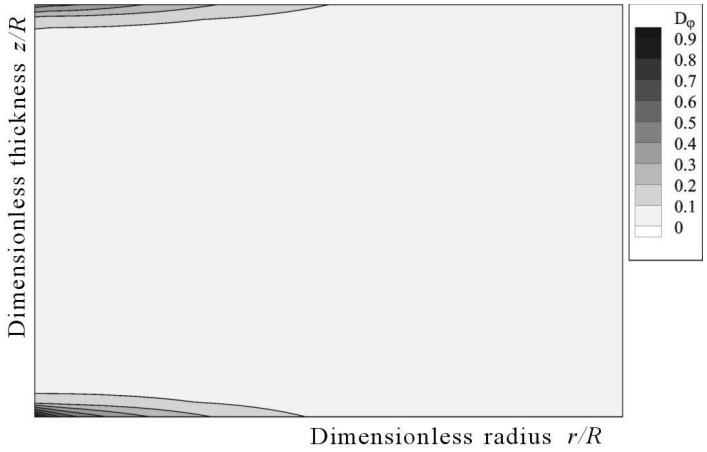

Fig. 4. Zone of hoop damage D_φ in plate under mechanical cyclic load $\pm p$

The radial damage component D_r grows with a lower rate in this case. Note, that the damage distributions at the top and bottom surfaces are not strictly symmetric because the most damaged zone (bottom) corresponds to the first downward loading cycle. The damage evolution at the bottom surface centre $D_\varphi^{(bottom)}$, compared to the top surface $D_\varphi^{(top)}$ is sketched in Fig. 5.

The damage growth is observed only under the maximum tensile principal stress σ_1, according to the simplified Hayhurst stress function $\chi(\boldsymbol{\sigma}) = \sigma_1$ used in (4.3) for copper. Damage cumulation at the bottom surface precedes that at the top one due to the downward first loading cycle. The displacement response of the plate measured at the center point of the middle surface $w(r = 0, z = 0)$ is schematically shown in Fig. 6. Alternating displacement amplitudes are nearly symmetric around zero, and no cyclic kinematic effect is observed.

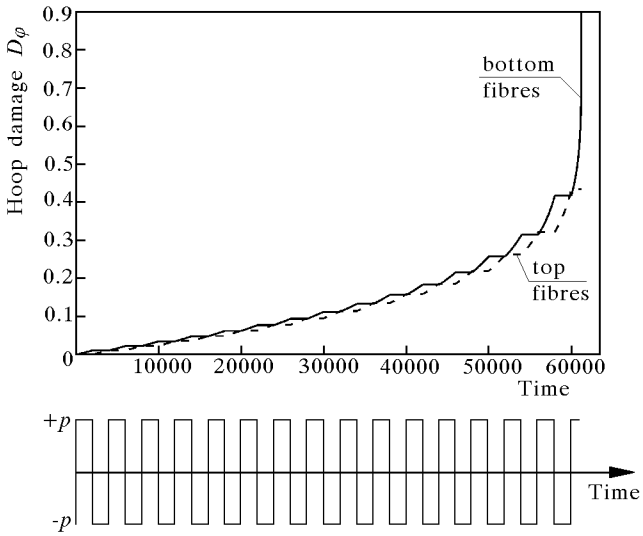

Fig. 5. Evolution of hoop damage D_φ in plate under mechanical cyclic load $\pm p$ at point of maximum damage

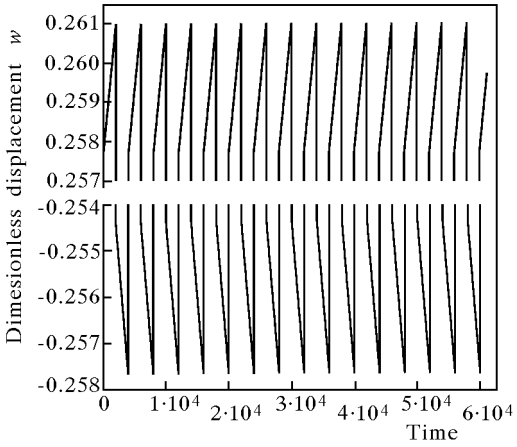

Fig. 6. Evolution of vertical displacement $w(r = 0, z = 0)$ at middle surface in plate under mechanical cyclic load $\pm p$

Plate response to combined mechanical reverse cyclic $\pm p$ and damage enhanced thermal $T(r, \mathbf{D})$ loads

In the following considerations, the plate is subjected to simultaneous reverse symmetric pressure cycles $p = \pm 0.1\sigma_0$ and affected the damage changeable temperature field $T(r, \mathbf{D})$ which is generated by the point heat source

(Fig. 3). The effect of damage on the thermal conductivity tensor $\widetilde{\boldsymbol{\lambda}}(\mathbf{D})$ is given by (3.7), where it is assumed that the elastic constitutive tensor $\mathbf{E}$ is not affected by damage. In contrast to the previous example, the plate simply heated by the point source is under "semi-membrane" compressive stress, the magnitude of which is the highest in the central part of the plate. Hence, the tensile stress-controlled damage is localized in this case at the plate sidewall around the bottom corner (cf. Ganczarski, 2001b). However, under a complex loading, if the plate is simultaneously subjected to both non-uniform temperature field and mechanical loading cycles, an additional damage localization zone appears at the top corner of the sidewall (Fig. 7). Growth of the hoop damage component at the top corner takes place when the mechanical and thermal displacement responses coincide $(-p$ in Fig. 8).

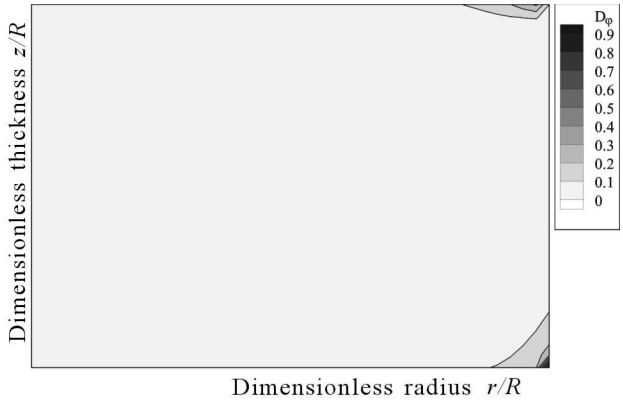

Fig. 7. Zone of hoop damage D_φ in plate under combined cyclic mechanical load $\pm p$ and damage enhanced thermal load $T(r, \mathbf{D})$

In other case $(+p$ in Fig. 8), the damage growth at the top becomes passive, whereas at the bottom the damage growth due to the thermal stress is enhanced by the additional mechanical effect (Fig. 8). The damage accumulation causes the essential decrease of the hoop component of thermal conductivity (3.7) however the hoop direction is not active in the modified heat transfer equation, whereas $D_r = D_z = \eta D_\varphi$, and consequently, the change of the local heat flux is rather small (Fig. 9).

In the considered case, the displacement response of the plate to its loading measured at the central point of the middle surface $w(r = 0, z = 0)$ is strongly non-symmetric in a way such that the plate curvature drops from cycle to cycle (Fig. 10). It is mainly due to creep during positive $(+p)$ loading cycles which is faster than that during negative ones $(+p)$. The process is terminated when the critical damage is met at the bottom sidewall corner, as seen in Fig. 7.

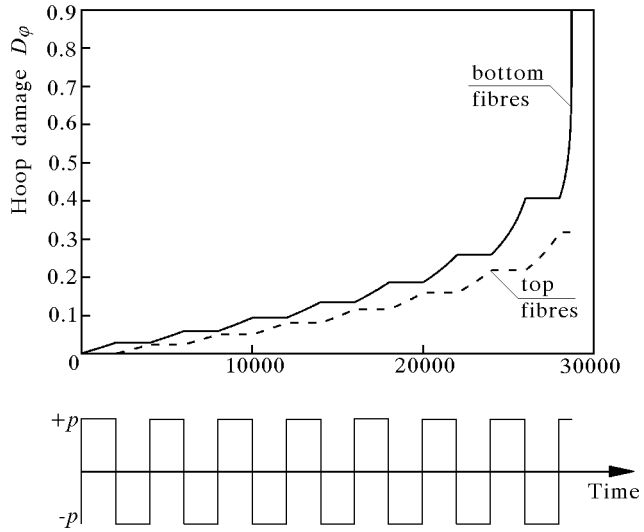

Fig. 8. Evolution of hoop damage D_φ in plate under mechanical cyclic load $\pm p$ and damage enhanced thermal load $T(r, \mathbf{D})$ at point of maximum damage

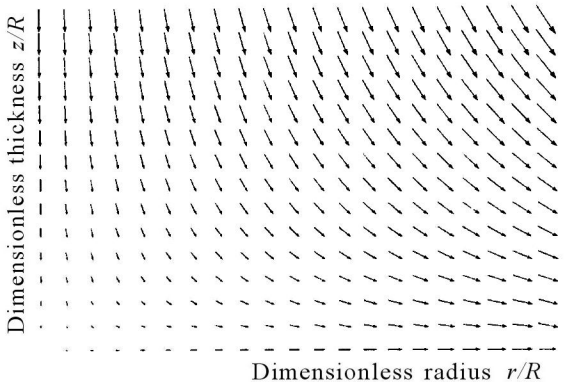

Fig. 9. Local heat flux $-\lambda_0(\mathbf{1} - \mathbf{D}) \cdot \operatorname{grad} T$

8. Conclusions

- When thermo-mechanical loadings are considered, coupled mechanical creep-damage and heat flux equations result in a damage induced anisotropy. If cyclic thermo-mechanical loadings are considered, an additional effect of damage deactivation must be included.

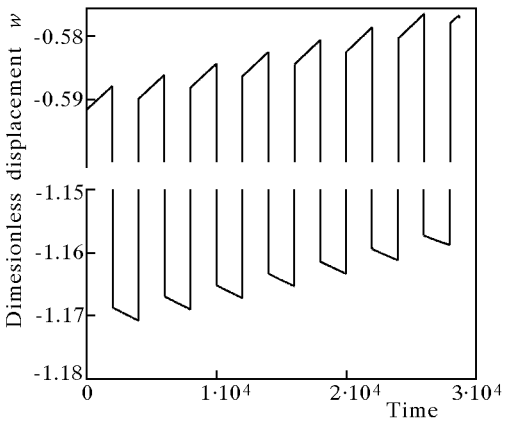

Fig. 10. Evolution of vertical displacement $w(r=0,z=0)$ at middle surface in plate under combined cyclic mechanical load $\pm p$ and damage enhanced thermal load $T(r,\mathbf{D})$

- A consistent formulation requires that the damage deactivation effect influences not only the creep-damage constitutive equations but also the damage induced anisotropic elasticity law and the anisotropic heat flux equation of damaged materials (modified Fourier equation).

- The damage deactivation effect on the creep-damage equation is incorporated by the extended definition of the effective stress for unilateral damage conditions (2.3).

- The elasticity law for the unilateral damage conditions can be introduced by applying modified effective elastic moduli $\widetilde{\mathbf{E}}^{+}$ or $\widetilde{\mathbf{E}}^{-}$ for active or passive damage conditions, respectively (Foryś and Ganczarski, 2002).

- The heat flux equation for the unilateral damage conditions should allow for not only a drop in the thermal conductivity with damage growth, but also for the conductivity recovery in crack closure phenomena.

References

1. CHABOCHE J.-L., 1992, Damage induced anisotropy: On the difficulties associated with the active/passive unilateral condition, *Int. J. Damage Mech.*, **1**, 2, 148-171

2. CHABOCHE J.-L., 1993, Development of continuum damage mechanics for elastic solids sustaining anisotropic and unilateral damage, *Int. J. Damage Mech.*, **2**, 311-329

3. CHABOCHE J.-L., LESNE P.M., MOIRE J.F., 1995, Continuum damage mechanics, anisotropy and damage deactivation for brittle materials like concrete and ceramic composites, *Int. J. Damage Mech.*, **4**, 5-21

4. FORYŚ P., GANCZARSKI A., 2002, Modelling of microcrack closure effect, *Proc. Int. Symp. "Anisotropic Behaviour of Damaged Materials"*, Kraków, (on CD)

5. GANCZARSKI A., 2001a, Acquired anisotropy accompanying coupled thermo-damage fields in 3D structures, *Proc. Thermal Stresses'01*, 363-366

6. GANCZARSKI A., 2001b, Computer simulation of transient thermo-damage fields in 3D structures, *Proc. ECCM-2001* (on CD ROM)

7. GANCZARSKI A., SKRZYPEK J., 2001, Application of the modified Murakami's anisotropic creep-damage model to 3D rotationally-symmetric problem, *Technische Mechanik*, **21**, 4, 251-260

8. HALM D., DRAGON A., 1996, A model of anisotropic damage by mesocrack growth; unilateral effect, *Int. J. Damage Mechanics*, **5**, 384-402

9. HALM D., DRAGON A., 1998, An anisotropic model of damage and frictional sliding for brittle materials, *Eur. J. Mech. A/Solids*, **17**, 3, 439-460

10. HANSEN N.R., SCHREYER H.L., 1995, Damage deactivation, *J. Appl. Mech.*, **62**, 450-458

11. HAYAKAWA K., MURAKAMI S., 1997, Thermodynamical modeling of elastic-plastic damage and experimental validation of damage potential, *Int. J. Damage Mech.*, **6**, 333-363

12. JU J.W., 1989, On energy based coupled elastoplastic damage theories: constitutive modeling and computational aspects, *Int. J. Solids and Structures*, **25**, 7, 803-833

13. KAVIANY M., 1995, *Principles of Heat Transfer in Porous Media*, Springer

14. KRAJCINOVIC D., 1996, *Damage Mechanics*, Elsevier, Amsterdam

15. KRAJCINOVIC D., FONSEKA G.U., 1981, The continuous damage theory of brittle materials, Part I and II, *J. Appl. Mech.*, ASME, **18**, 809-824

16. LADEVEZE P., LEMAITRE J., 1984, Damage effective stress in quasi-unilateral conditions, *Proc. IUTAM Congr.*, Lyngby, Denmark

17. LITEWKA A., 1991, *Creep Damage and Creep Rupture of Metals*, Wyd. Polit. Poznańskiej, (in Polish)

18. LUBARDA V.A., KRAJCINOVIC D., MASTILOVIC S., 1994, Damage model for brittle elastic solids with unequal tensile and compressive strength, *Eng. Fracture Mech.*, **49**, 5, 681-697

19. MAZARS J., 1986, A model of unilateral elastic damageable material and its application to concrete, In: *Energy Toughness and Fracture Energy of Concrete*, F.H. Wittmann (Ed.), Elsevier Sci. Publ., Amsterdam, The Netherlands, 61-71

20. MURAKAMI S., KAMIYA K., 1997, Constitutive and damage evolution equations of elastic-brittle materials based on irreversible thermodynamics, *Int. J. Solids Struct.*, **39**, 4, 473-486

21. MURAKAMI S., KAWAI M., RONG H., 1988, Finite element analysis of creep crack growth by a local approach, *Int. J. Mech. Sci.*, **30**, 7, 491-502

22. PRESS W.H., TEUKOLSKY S.A., VETTERLING W.T., FLANNERY B.P., 1993, *Numerical Recipes in Fortran*, Cambridge Press

23. RAMTANI S., 1990, Contribution á la Modelisation du Comportement Multiaxial du Beton Endommagé avec Description du Caractere Unilateral, PhD Thesis, Univ. Paris VI

24. SKRZYPEK J.J., KUNA-CISKAŁ H., 2003, Anisotropic elastic-brittle-damage and fracture models based on irreversible thermodynamic, In: *Anisotropic Behaviour of Damaged Materials*, J.J. Skrzypek and A. Ganczarski (Eds), Springer-Verlag, Berlin-Heidelberg, 143-184

Modelowanie uszkodzenia przy pełzaniu w grubych płytach poddanych cyklicznym obciążeniom termomechanicznym

Streszczenie

Praca będąca rozwinięciem poprzednich artykułów autorów jest poświęcona sprzężeniu efektów termicznych oraz pełzania z uszkodzeniem występującym w trójwymiarowych konstrukcjach obrotowo-symetrycznych poddanych działaniu cyklicznie zmiennych złożonych obciążeń termomechanicznych. Sprzężenie efektów termicznych i uszkodzenia opisane jest zmodyfikowanym prawem Fouriera, w którym tensor przewodności termicznej jest uzależniony od tensora uszkodzenia. Efekt otwierania/zamykania mikroszczelin jest uwzględniony w równaniach konstytutywnych poprzez wprowadzenie oddzielnych definicji naprężenia efektywnego dla rozciągania i ściskania. Pozwala to uwzględnić niezupełną deaktywację uszkodzenia, opisaną diagonalnym tensorem zamknięcia mikroszczelin, towarzyszącą naprzemiennym cyklom obciążenia. Ewolucja uszkodzenia podlega mieszanemu izotropowo/anizotropowemu prawu typu Murakami, w którym wprowadzono modyfikację mającą na celu usunięcie

niejednoznaczności rozwiązania, która jest związana z opisem wzrostu uszkodzenia w konstrukcjach o obrotowej symetrii. Sprzężenie procesów pełzania i uszkodzenia podlega równaniom typu Murakami przystosowanym do opisu obciążeń cyklicznych. Jako przykład zaprezentowano analizę uszkodzenia w trójwymiarowej płycie poddanej obciążeniom termomechanicznym polegającym na równoczesnym działaniu niejednorodnego pola temperatury pochodzącego od punktowego źródła ciepła usytuowanego ponad górną powierzchnią płyty oraz naprzemiennie zmiennego równomiernego ciśnienia.

Manuscript received March 1, 2004; accepted for print April 23, 2004